

Date of publication xxxx 00, 0000, date of current version xxxx 00, 0000.

Digital Object Identifier 10.1109/ACCESS.2017.Doi Number

A New Dispersion Control Chart for Handling the Neutrosophic Data

Zahid Khan¹, Muhammad Gulistan¹, Wathek Chamam², Seifedine Kadry³, Yunyoung Nam⁴

¹Department of Mathematics and Statistics, Hazara University Mansehra, Pakistan

²Department of Mathematics, College of Science Al-Zulfi, Majmaah University, Al-Zulfi, Saudi Arabia

³Department of Mathematics and Computer Science, Faculty of Science, Beirut Arab University, Lebanon

⁴Department of Computer Science and Engineering, Soonchunhyang University, Asan 31538, Korea

Corresponding authors: W. Chamam (e-mail: c.chamam@mu.edu.sa) and Y. Nam (e-mail: ynam@sch.ac.kr)

This research was supported by the Ministry of Trade, Industry & Energy (MOTIE), Korea Institute for Advancement of Technology (KIAT) through the Encouragement Program for The Industries of Economic Cooperation Region (P0006082) and also supported by the Soonchunhyang Research Fund.

ABSTRACT The control chart based on mean deviation (MD) is customary used as a robust alternative to the existing Shewhart control charts for observing changes in dispersion parameter of the process. The existing model of MD control chart is rooted under the assumption that indeterminate observations are not included in measured quality characteristic. If, inspected quality data entail some indeterminate and vague information, typical design of the MD control chart could not be effectively employed. This study originally presents an appropriate generalized design namely neutrosophic mean deviation (\widetilde{MD}) control chart that could accommodate imprecise observations in collected quality characteristic variables. Under the neutrosophic situation, the related properties of this newly \widetilde{MD} design have been derived. Using simulated data, performance of the \widetilde{MD} control chart in terms of neutrosophic average run length (\widetilde{ARL}) is investigated. The performance of proposed \widetilde{MD} control chart relative to existing competitor designs has been evaluated. The study reveals that proposed design of \widetilde{MD} chart outperforms as to existing counterparts in terms of statistical power. To illustrate the efficacy of this new design, real data from a manufacturing company has been used to describe the control procedure of the proposed \widetilde{MD} control chart.

INDEX TERMS Fuzzy control charts, probability limits, mean deviation, neutrosophic data, variability control charts

I. INTRODUCTION

The existence of normal variation in almost every manufactured item is the most likely phenomenon due to different inherent factors. In statistical procedures, control chart approach is used as one of primary tools to study different variability components so that abnormal variation, resulting from different causing factors can be pinpointed [1]. Currently, control charts are extensively employed as a statistical procedure, particularly in industries to identify the contributing factors of normal and abnormal variation in manufactured products in view of some quality characteristics. In quality control frameworks, measured quality characteristic variables are assumed to be stable both in the location and scale parameters because unfavorable changes significantly effect on these distribution parameters of quality characteristic measurements [2]. The process average and variability are therefore needed to be controlled by using variety of charts available in literature. In back, 1920s, Shewhart proposed a variety of control charts for

observing stability in mean and process variability [3]. The R chart is based on simplest statistical measure namely range (R) and S chart rooted on a relatively good measure of variability called standard deviation (S). Both primary charts are generally suggested for observing the process variability [4]. Additionally, R chart is inferior in view of losing efficiency for smaller sample size and wasting data information in its calculation. In contrast, the underlying statistic of S control chart is not a robust measure of variability and becomes greatly influenced by existence of outliers in data [5]. In many realistic situations where data with tiny errors are processed, the MD statistic which is another dispersion measure has advantage over the traditional S statistic as mentioned in [6]. The mean deviation has a variety of versions in which deviation from median is not potentially influenced by outliers in the processing data [7]. The MD measure is superior to S in contaminated situations in the processing data [8].

Dealing with empirical data, while employing MD statistic occasionally works better than S [9]. The MD is not consistently efficient than S statistic under ideal assumption of perfect normal distribution [10]. Many realistic situations require assumption of normality that is not being met [11]. Due to this apparent superiority of MD statistic, Riaz and Saghir [6] presented MD control chart for dispersion monitoring. Based on other related measures many researchers proposed various control charts for monitoring the dispersion parameter of the process details on which can be seen in [12]. The design of Shewhart-type control charts is found on notion of crisp data that are not always available in some real situations [13]. The imprecision in distribution parameters or vagueness in measured quality characteristics may result in uncertainty environment. In such scenarios, dealing with traditional control chart approach is not applicable however; it becomes necessary for control chart practitioners to construct fuzzy structure for the control charts in order to accommodate indeterminacy in data. Sabegh et al. [14] presented extensive overview of the fuzzy control charts.

The classical set logic is further extended to instituted and subsequently neutrosophic set by incorporating indeterminacy as an independent membership component [15]. In practical applications, assumption of exact values available for computing quality characteristics is not likely to be met [16]. Smarandache [17] initially interpreted an idea of neutrosophic data which is an extension of classical data. As a result, many researchers working in the field of quality control also introduced generalized design structures of many existing control charts which allow dealing vague data information on the studied variables. First time, Asalm introduced the applications of the neutrosophic statistics in the field of statistical quality control [18]. Recently, Aslam and Khan designed the

neutrosophic version of X -bar chart for monitoring the indeterminate mean parameter of the process [19]. The neutrosophic S^2 control chart for observing the scale parameter is given in the work [20]. Under neutrosophic and repetitive sampling scenarios attribute control chart has been established in [21]. There are many other neutrosophic version of well documented control charts and related areas, details on which can be found in references [22]–[27].

This study develops a new variability control chart namely a \widetilde{MD} under the assumption that imprecise observations are encountered in the processing data and exact values are not readily available. The propose design of \widetilde{MD} represents a generalized structure and coincides with the existing design of the MD control chart under zero indeterminacy in processing data and design parameters.

The remainder of paper is outlined in sections as follows. The proposed design of \widetilde{MD} control chart is presented in Section II. Section III, illustrates the monitoring process of \widetilde{MD} control chart and covers the related concept of the \widetilde{ARL} using simulated data. The usefulness of proposed chart with other competitor designs is provided in Section IV. Section V, demonstrates the set-up procedure of \widetilde{MD} control chart on real data case in details. Eventually, Section VI concludes the findings of the study.

II. PROPOSED DESIGN

The proposed design of \widetilde{MD} control chart is relying on the assumption that an indeterminate random sample $\tilde{n} \in [n_L, n_U]$ is taken from the neutrosophic normal distribution with imprecise parameter values $\tilde{\mu} \in [\mu_L, \mu_U]$ and $\tilde{\sigma} \in [\sigma_L, \sigma_U]$. The neutrosophic distribution is an extended form of the classical normal distribution [26]. For instant, neutrosophic normal density curves for various imprecise parameters are portrayed in Figure 1.

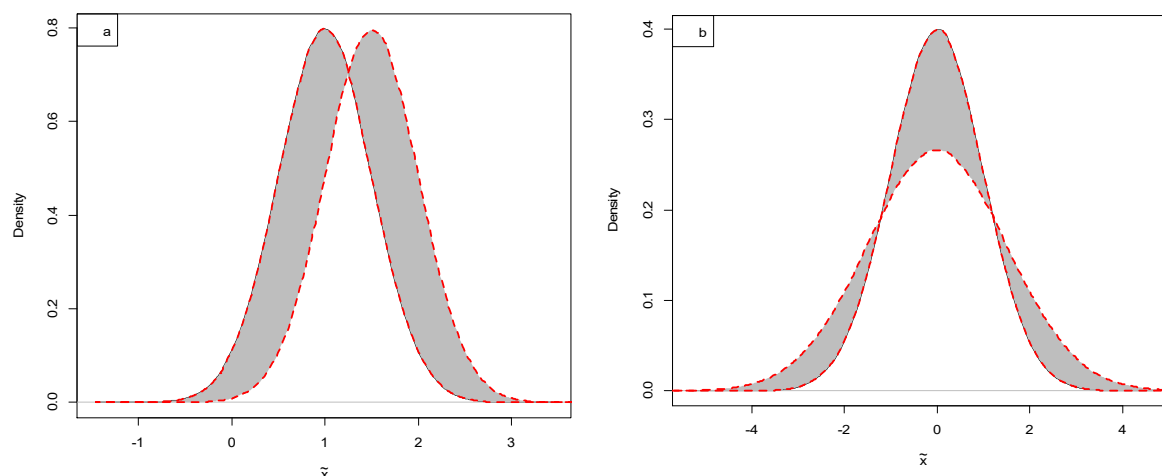


FIGURE 1. Neutrosophic normal distribution (a) with imprecise mean, $\tilde{\mu} = [1, 2.5]$ (b) with imprecise standard deviation, $\tilde{\sigma} = [1, 1.5]$

Figure 1 (a) shows that distribution is stable at precise shape parameter which is equal to 1 but, the mean is indeterminate and varies in range [1, 2.5] whereas Figure 1(b) shows distribution with indeterminate standard deviation that varies in range [1, 1.5]. In each graph, shaded area between the curves represents indeterminate region of the neutrosophic normal distribution. This example illustrates the idea behind the neutrosophic normal distribution. Similarly, distribution with both neutrosophic parameters can be established.

The proposed chart utilizes the \widehat{MD} which is defined for neutrosophic random sample of size \tilde{n} as:

$$\widehat{MD} = \frac{\sum_{i=1}^{\tilde{n}} |\tilde{x}_i - \tilde{m}|}{\tilde{n}}, \quad \tilde{m} \in [m_L, m_U], \quad \tilde{n} \in [n_L, n_U] \quad (1)$$

where \tilde{m} is sample neutrosophic median.

Equation (1) represents the neutrosophic mean deviation based on neutrosophic random sample and is a robust measure of process variability.

Let the quality characteristic say W follows the neutrosophic normal distribution $N(\tilde{\mu}, \tilde{\sigma}^2)$. To derive the proposed chart, it is required to define the relationship between \widehat{MD} and unknown but true value of neutrosophic dispersion parameter $\tilde{\sigma}$. Let a neutrosophic random sample $\tilde{x}_1, \tilde{x}_2, \dots, \tilde{x}_{\tilde{n}}$ is taken from $N(\tilde{\mu}, \tilde{\sigma}^2)$ and neutrosophic random variable \tilde{T} represents the required relationship as:

$$\tilde{T} = \frac{\widehat{MD}}{\tilde{\sigma}}, \quad \tilde{T} \in [T_L, T_U]. \quad (2)$$

The distributional curve of the neutrosophic test statistic \tilde{T} exclusively depends on the neutrosophic sample size \tilde{n} . For smaller sample size; the distribution behavior of \tilde{T} statistic is not symmetric even for the normally distributed quality characteristic. In order to meet the general model of the Shewhart control chart for the neutrosophic data, it is required to derivate the mean and standard deviation of the statistic defined in (2).

Taking expectation, (2) provides

$$E(\tilde{T}) = \frac{E(\widehat{MD})}{\tilde{\sigma}}. \quad (3)$$

For in-control process, $E(\widehat{MD})$ can be replaced safely by an estimate $\widehat{\widehat{MD}}$, the mean of all neutrosophic samples for the quality characteristic under study.

Thus (3) implies that:

$$\hat{\sigma} = \frac{\widehat{\widehat{MD}}}{E(\tilde{T})} \quad (4)$$

$$\text{Let } E(\tilde{T}) = \tilde{t}_2, \quad \tilde{t}_2 \in [t_{2L}, t_{2U}]. \quad (5)$$

Equation (5) represents the mean of the neutrosophic test statistic \tilde{T} which is difficult to derive analytically due to unclosed form of the integral for the normal density function. However, simulation results as provided in [6] can be utilized for finding the value of \tilde{t}_2 for different sample size ranges.

Thus from (4), it is obvious that

$$\hat{\sigma} = \frac{\widehat{\widehat{MD}}}{\tilde{t}_2}. \quad (6)$$

The expression for $\hat{\sigma}$ in (6) is similar to the estimate of σ used in R and S control charts for dispersion monitoring [28].

Moreover, for the required standard error it has been supposed that

$$\sigma_{\tilde{T}} = \tilde{t}_3, \quad \tilde{t}_3 \in [t_{3L}, t_{3U}] \quad (7)$$

Again, with difficulty in analytically solution the simulation results can be set-up to find the values of \tilde{t}_3 for different values of neutrosophic sample size.

Thus the variance of neutrosophic random variable \tilde{T} from (2) can be written as:

$$\sigma_{\tilde{T}} = \frac{\sigma_{\widehat{MD}}}{\tilde{\sigma}}, \quad (8)$$

where $\sigma_{\widehat{MD}}$ represents the neutrosophic standard error of the distribution of the statistic \widehat{MD} .

From (7) and (8), the estimate of $\sigma_{\widehat{MD}}$ can be written as:

$$\hat{\sigma}_{MD} = \widehat{\widehat{MD}} \frac{\tilde{t}_3}{\tilde{t}_2}. \quad (9)$$

Thus, the neutrosophic parameters (i.e., LCL , CL and UCL) of the proposed control charts by using the Shewhart's general model can be expressed as:

$$\left. \begin{aligned} UCL &= \widehat{\widehat{MD}} + 3\widehat{\widehat{MD}} \frac{\tilde{t}_3}{\tilde{t}_2} \\ CL &= \widehat{\widehat{MD}} \\ LCL &= \widehat{\widehat{MD}} - 3\widehat{\widehat{MD}} \frac{\tilde{t}_3}{\tilde{t}_2} \end{aligned} \right\} \quad (10)$$

where $\widehat{\widehat{MD}} \in [\widehat{\widehat{MD}}_L, \widehat{\widehat{MD}}_U]$, $\tilde{t}_2 \in [t_{2L}, t_{2U}]$ and $\tilde{t}_3 \in [t_{3L}, t_{3U}]$.

The validity of limits given in (10) is based on the assumption that quality characteristic under study follows the approximate neutrosophic normal distribution. However, the true distribution of \tilde{T} is not symmetric for smaller sample size. Therefore the probability limits are realistic choice in real applications where generated data is not necessary from the assumed model [29].

Using the classical structures of probability limits for R , S and G control charts, the probability limits of the proposed neutrosophic designed then leads to:

$$UCL = \tilde{T}_R \hat{\sigma} \text{ with } P(\tilde{T} \leq \tilde{T}_R) \geq 1 - \alpha_R \quad (11)$$

$$LCL = \tilde{T}_L \hat{\sigma} \text{ with } P(\tilde{T} \leq \tilde{T}_L) \leq \alpha_L$$

where $\alpha = \alpha_L + \alpha_R$, is the specified type-I error, divided in right (α_R) and left (α_L) tail probability, $\hat{\sigma}$ is estimated from subgroups data using eq (6), \tilde{T}_L and \tilde{T}_R are percentage points of the \tilde{T} distribution at the specified value of n .

Thus (10) and (11) can be used to construct desired neutrosophic control limits of the \widehat{MD} control chart. However, the LCL in 3-sigma limits sometimes set zero for negative values of LCL at small values of \tilde{n} which is unrealistic meaning in case of dispersion measure. On other hand, probability limits given as defined in (11), always have a value for LCL , hence are much more effective than conventional 3-sigma limits. The average run length (ARL) for the proposed chart based on probability limits can be derived.

Likewise, the neutrosophic structure of ARL has been used in many recent studies for assessing the performance of proposed control charts [30]. The $\widetilde{ARL} \in [\widetilde{ARL}_L, \widetilde{ARL}_U]$ for proposed \widetilde{MD} -chart can be determined.

According to classical defined of ARL [31], \widetilde{ARL} for in control process can be defined as:

$$\widetilde{ARL}_0 = \frac{1}{\alpha} \quad (12)$$

where $\alpha = 1 - Pr[LCL \leq \widetilde{MD}_i \leq UCL]$ is the probability of exceeding \widetilde{MD}_i from the constructed neutrosophic control limits.

Considering (11) and simplifying (3) implies:

$$\begin{aligned} Pr[LCL \leq \widetilde{MD}_i \leq UCL] \\ = Pr[\widetilde{MD}_i \leq \widetilde{T}_R \hat{\sigma}] - Pr[\widetilde{MD}_i \leq \widetilde{T}_L \hat{\sigma}] \end{aligned}$$

Hence equation (12) becomes

$$\widetilde{ARL}_0 = \frac{1}{1 - Pr[\widetilde{MD}_i \leq \widetilde{T}_R \hat{\sigma}] + Pr[\widetilde{MD}_i \leq \widetilde{T}_L \hat{\sigma}]} \quad (13)$$

When the process is shifted to out of control state i.e., $\tilde{\sigma}_1 = \Delta \tilde{\sigma}_0$, with shift constant $\Delta > 1$ then

$$\widetilde{ARL}_1 = \frac{1}{1 - \beta} \quad (14)$$

where $\beta = Pr[\widetilde{MD}_i \leq \widetilde{T}_R \hat{\sigma} | \tilde{\sigma}_1] - Pr[\widetilde{MD}_i \leq \widetilde{T}_L \hat{\sigma} | \tilde{\sigma}_1]$ is probability under the alternative hypothesis that process has been shifted to new standard deviation $\tilde{\sigma}_1$.

The ARL is an important indicator for measuring the performance of control charts. It has been used in the Section III for assessing the performance of \widetilde{MD} control chart.

III. PROCESS MONITORING USING SIMULATED DATA

To monitor the scale parameter $\tilde{\sigma}$ using the proposed chart depends upon the construction of conventional 3-sigma limits \widetilde{UCL} and \widetilde{LCL} defined in equation (10) and in case of probability limits, control limits defined in equation (11) would be used. The process is assumed to be working in a control state with scale parameter $\tilde{\sigma}_0$. Now it has been assumed that process is shifted to the new state with a scale parameter $\tilde{\sigma}_1 = \Delta \tilde{\sigma}_0$ where $\Delta \geq 1$ is a shift constant. Note here, $\Delta = 1$ implies that process is stable at the value of monitoring parameter $\tilde{\sigma}_0$. If the quality of the observed process has been declined by the amount Δ i.e., $\Delta > 1$, how many expected number of samples immediately following this change are required to detect the shift. This would result in the sensitivity of the proposed chart against this shift and measure in terms of \widetilde{ARL}_1 . Now, we define all parameters given in (14) in order to obtain the \widetilde{ARL}_1 for the proposed chart. To this, let preliminary specify in control $\widetilde{ARL}_0 \in [500, 500]$ and \tilde{n} belongs to different range of sample sizes says $\tilde{n} \in [2, 4]$ and $\tilde{n} \in [8, 10]$. Total 10000 simulated random samples each of size \tilde{n} have been generated from the neutrosophic normal distribution with indeterminate parameter $\tilde{\mu} = \{0, 0.5\}$ and $\tilde{\sigma} = \{1, 1\}$. From each sample, \widetilde{MD}_i has been obtained. For each neutrosophic

sample size \tilde{n} , quantiles points of \tilde{T} distribution are obtained for subsequent used in control limits that based on probability limits approach as defined in (11). The resulting \widetilde{ARL}_1 values for \widetilde{MD} -chart at different values of the shift constant Δ are computed and displayed in Table 1 and Table 2.

TABLE 1. THE VALUES OF \widetilde{ARL}_1 OF THE \widetilde{MD} CONTROL CHART WITH $\widetilde{ARL}_0 \in [100, 100]$

| Δ | \widetilde{ARL}_1 | |
|----------|------------------------|-------------------------|
| | $\tilde{n} \in [2, 4]$ | $\tilde{n} \in [8, 10]$ |
| 1 | [101.11, 103.73] | [89.04, 100.21] |
| 1.5 | [57.57, 112.11] | [12.27, 18.29] |
| 2 | [25.54, 86.65] | [2.94, 4.73] |
| 2.5 | [14.06, 73.42] | [1.48, 2.16] |
| 3 | [8.54, 57.67] | [1.11, 1.41] |
| 2.5 | [5.85, 51.09] | [1.02, 1.14] |
| 4 | [4.25, 43.59] | [1.00, 1.04] |
| 4.5 | [3.28, 39.53] | [1.00, 1.01] |
| 5 | [2.63, 35.07] | [1.00, 1.00] |

TABLE 2. THE VALUES OF \widetilde{ARL}_1 OF THE \widetilde{MD} CONTROL CHART WITH $\widetilde{ARL}_0 \in [500, 500]$

| Δ | \widetilde{ARL}_1 | |
|----------|------------------------|-------------------------|
| | $\tilde{n} \in [2, 4]$ | $\tilde{n} \in [8, 10]$ |
| 1 | [462.96, 520.83] | [438.59, 506.27] |
| 1.5 | [209.21, 512.82] | [34.72, 62.93] |
| 2 | [86.51, 398.41] | [6.21, 13.61] |
| 2.5 | [46.25, 320.51] | [2.36, 4.79] |
| 3 | [28.17, 243.90] | [1.42, 2.48] |
| 2.5 | [18.48, 210.52] | [1.12, 1.63] |
| 4 | [12.55, 173.01] | [1.03, 1.27] |
| 4.5 | [9.10, 163.27] | [1.00, 1.11] |
| 5 | [6.95, 146.19] | [1.00, 1.04] |

control value of the average length i.e., $\widetilde{ARL}_0 = 500$, is always attended and remains within the computed interval. Note that if the process shifted by the amount 1.5Δ using neutrosophic sample $[2, 4]$, on average $[57.57, 112.11]$ number of samples are required to detect this shift. In general, it is obvious from Table 1 that at fixed value of \tilde{n} , the \widetilde{ARL}_1 value decreases as the value of shift constant Δ increased which indicates that large shift is reasonably more quickly detected by the proposed chart. Moreover, \widetilde{ARL}_1 value at larger sample size approaches to unity with the increased of shift constant Δ . Therefore, the proposed chart is reasonably sensitive to larger and moderate shifts in the process.

Similar conclusion can be followed from the results reported in Table 2.

In addition to \widetilde{ARL} , neutrosophic characteristic curve (\widetilde{OC}) can be occasionally established to describe the ability of control for detecting the shift in the process. In order to construct \widetilde{OC} curve for the proposed chart we assume the following hypothesis is being testing at specific value of α for the observed process:

$\widetilde{H}_0: \tilde{\sigma} = \tilde{\sigma}_0$ i.e., process is in control at scale parameter $\tilde{\sigma}_0$.

$\widetilde{H}_1: \tilde{\sigma} = \tilde{\sigma}_1 = \Delta\tilde{\sigma}_0$ i.e., process is shifted at scale parameter $\tilde{\sigma}_1$.

Now the construction of \widetilde{OC} curve involves the probability of type-II error (β) which is defined for proposed chart in term of probability limits as:

$$\beta = Pr[\widetilde{MD}_i \leq \widetilde{T}_R \hat{\sigma} | \tilde{\sigma}_1] - Pr[\widetilde{MD}_i \leq \widetilde{T}_L \hat{\sigma} | \tilde{\sigma}_1]. \quad (15)$$

Equation (15) denotes the probability of accept the null false null hypothesis i.e., in fact process has been moved to new state with scale parameter $\tilde{\sigma}_1$ but we are committing the error by accept the null hypothesis that process is in control state with scale parameter $\tilde{\sigma}_0$. Using the same preceding simulated data, the \widetilde{OC} curves of the \widetilde{MD} control chart are constructed for different neutrosophic samples are displayed in Figure 2 below.

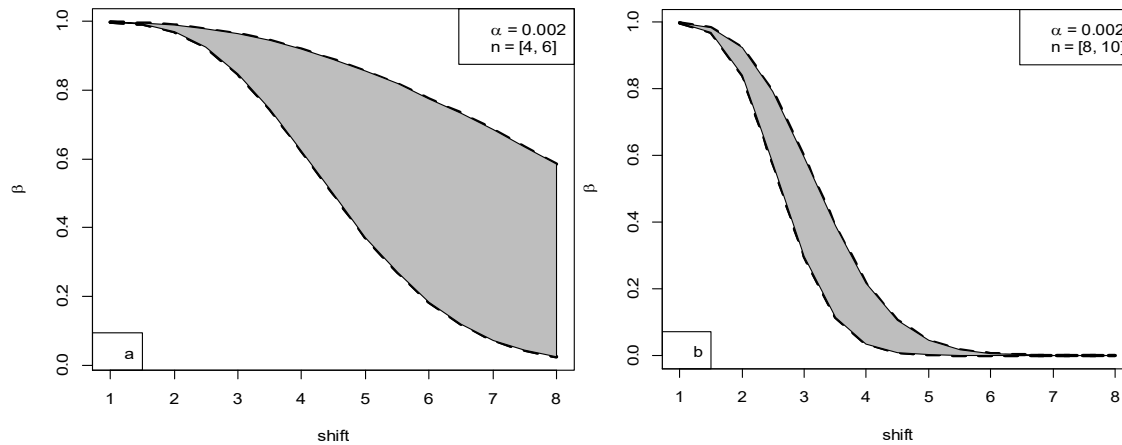


FIGURE 2. The \widetilde{OC} curves of \widetilde{MD} control chart at different neutrosophic sample size \tilde{n}

The \widetilde{OC} curves in Figure 2 show that as the process shifted from hypothesized value $\tilde{\sigma}_0$, the probability of committing the Type-II error decreased at a specific value of α and \tilde{n} . This means that the proposed chart will detect the larger shift more effectively as compared to smaller ones for given value of α and \tilde{n} . As the neutrosophic sample size increases, the probability β decreases for given value of α and \tilde{n} as shown in Figure 2(b). Accordingly, for larger sample sizes, the proposed control chart may become more powerful for detecting the shift of specific amount. For example, detecting the shift of 3 in Figure 2, the required power (i.e., $1 - \beta$) of \widetilde{MD} control chart belongs to intervals $[0.036, 0.153]$ and $[0.404, 0.703]$ for the neutrosophic samples $[4, 6]$ and $[8, 10]$ respectively. The neutrosophic area is represented by the shaded region in Figure 2. Thus, the power curves are useful for visualizing the particular shift with specific probability and can be computed for comparing the performance of proposed chart with another counterpart.

IV. COMPARISON WITH EXISTING CHARTS

In this section, performance analysis of the proposed control chart is given with other existing neutrosophic charts. As the \widetilde{MD} control chart belongs to the class of

charts usually used for monitoring the process variability, therefore, the comparison of the \widetilde{MD} control chart is given with other charts that are designed for variability monitoring under the neutrosophic environment. The neutrosophic design of the conventional R and S charts for monitoring the dispersion of the process exists in literature [19], [20]. Among the several statistical approaches, power curve is used as one of the effective tools for assessing the performance of different controls. The power of the proposed chart is defined as:

$$power = Pr[\widetilde{MD}_i > \widetilde{T}_R \hat{\sigma} | \tilde{\sigma}_1] - Pr[\widetilde{MD}_i < \widetilde{T}_L \hat{\sigma} | \tilde{\sigma}_1] \quad (16)$$

Equation (16) provides the probability of rightly rejecting the null hypothesis H_0 . In our situation, if the plotted statistics \widetilde{MD}_i goes beyond the lower and upper probability limits for given value of false alarm probability α and neutrosophic sample size \tilde{n} , it would constitute the power of the \widetilde{MD} control chart. Any control chart that provides greater probability of correctly rejecting H_0 , would be considered as an efficient approach for detecting the shift when in fact process has been shifted to new state with parameter $\tilde{\sigma}_1$. Employing this approach, power of the test for proposed chart and its counterparts R and S charts have been computed for fixed value of $\alpha = 0.002$.

To achieve the power curves, simulated data likewise the previous section have been generated at various neutrosophic sample sizes using software R.3.2.5. For given value of α and \tilde{n} , power curves of proposed chart in

comparisons with R and S charts are depicted in Figure 3 and Figure 4 respectively.

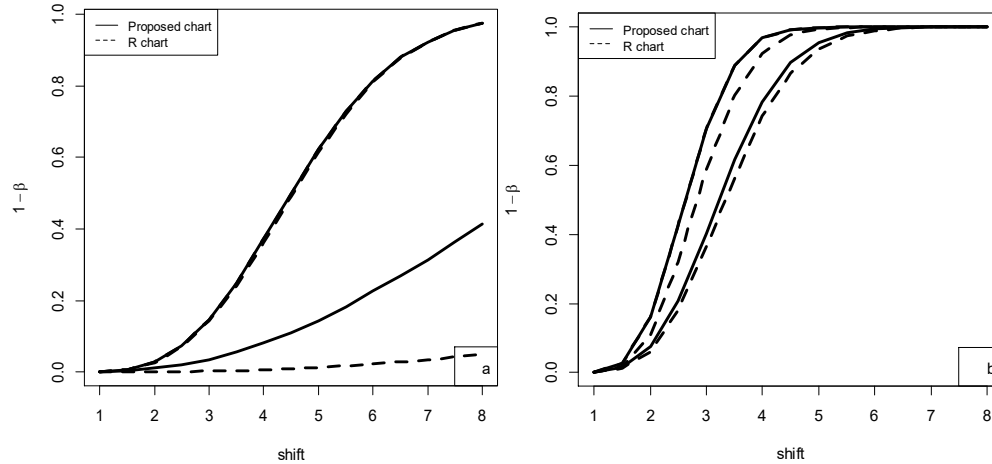


FIGURE 3. Neutrosophic power curves of \widehat{MD} control chart and R chart at (a) $\tilde{n} \in [4, 6]$ and $\alpha = 0.002$ (b) $\tilde{n} \in [8, 10]$ and $\alpha = 0.002$

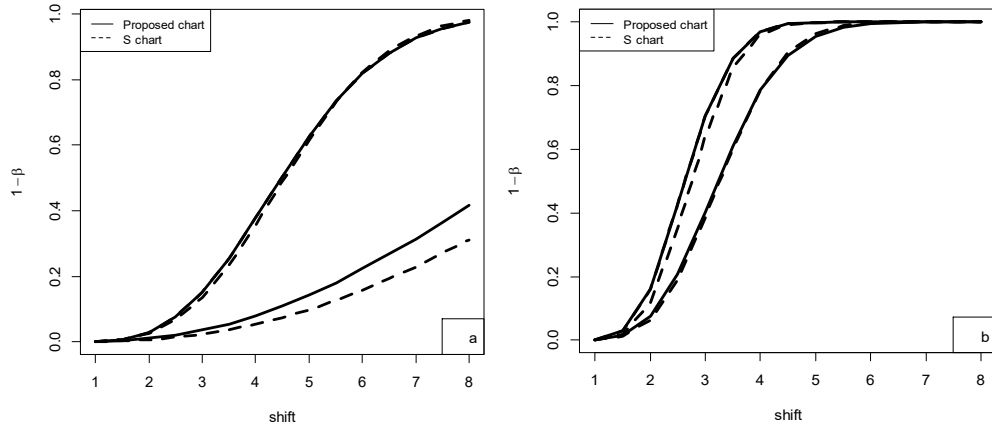


FIGURE 4. Neutrosophic power curves of \widehat{MD} control chart and S chart at (a) $\tilde{n} \in [4, 6]$ and $\alpha = 0.002$ (b) $\tilde{n} \in [8, 10]$ and $\alpha = 0.002$

Figure 3 and Figure 4 indicate that when process is in control with shift $\Delta = 1$, power is considerably closer to theoretical probability $\alpha = 0.002$. Whereas in case the process shifts to out of control state with $\Delta > 1$ at specific value of \tilde{n} , power of each control chart increases. However, clearly from Figure 3, that for given value of \tilde{n} , proposed \widehat{MD} control chart is more powerful than neutrosophic R chart for detecting shift in process parameter $\tilde{\sigma}_0$. For example, power of proposed \widehat{MD} control chart for shift, $\Delta = 5$ at $\tilde{n} \in [4, 6]$ is $[0.147, 0.621]$ which is greater than the corresponding power $[0.012, 0.613]$ of the neutrosophic R chart. The same is also true for other values of shift constant Δ as shown in Figure 3. In addition, power curves in Figure 3 are evaluated at small and large neutrosophic sample sizes which show that different behaviors of power curves between the proposed chart and neutrosophic R chart. Here the difference of power is larger at smaller neutrosophic sample in comparison to large sample size. Whereas, the performance of neutrosophic S control chart as shown in Figure 4, is slightly better than R chart and

closer to that of proposed \widehat{MD} control chart. However, overall performance of proposed chart substantially seems better than S chart across the various neutrosophic sample sizes. In addition to power curves, the performance of proposed design has been compared with the existing design of Riaz and Saghir [6] in relation to \widehat{ARL}_1 properties. The proposed design is set up for $\widehat{ARL}_0 \in [100, 100]$ in view to estimate the value of \widehat{ARL}_1 . The proposed control chart has been evaluated at assumed neutrosophic samples $\tilde{n} \in [2, 4]$ and $\tilde{n} \in [6, 8]$ while the existing MD control chart is constructed at average sample sizes 3 and 7. The estimated \widehat{ARL}_1 are presented in Table 3.

TABLE 3. PERFORMANCE OF THE PROPOSED DESIGN WITH EXISTING IN TERMS OF \bar{ARL}_1

| Shift constant Δ | \bar{ARL}_1 | |
|-------------------------|---|----------------------------|
| | Proposed design at $\tilde{n} \in [4, 6]$ | Existing design at $n = 5$ |
| 1 | [104.60, 108.70] | 103.63 |
| 1.5 | [38.15, 57.94] | 32.24 |
| 2.0 | [14.06, 25.87] | 10.21 |
| 2.5 | [6.91, 14.25] | 4.57 |
| 3.0 | [3.97, 8.74] | 2.62 |
| 3.5 | [2.67, 5.88] | 1.81 |
| 4.0 | [1.99, 4.25] | 1.43 |
| 4.5 | [1.60, 3.28] | 1.22 |
| 5.0 | [1.36, 2.62] | 1.11 |

The results given in Table 3 show that the conventional approach of the MD control chart provides \bar{ARL}_1 within the imprecise intervals resulted from the proposed approach. The design will be considered more adequate and effective if it provides estimates in indeterminate range rather than exact value under the uncertainty situations as described in [32]. It is also worth mentioned, results of the proposed design of \bar{MD} control chart coincide with the conventional MD control chart under zero indeterminacy i.e., $\mu_L = \mu_U = \mu$, $\sigma_L = \sigma_U = \sigma$, $ARL_L = ARL_U = ARL$, and $n_L = n_U = n$. Moreover, the neutrosophic \bar{ARL} value calculated previously is a function of some assumed constant values of the design parameters and shift amount.

In real-life circumstances, these parameters and shift constant are not known in advance [33]. Therefore some researchers recommend to use the ARL as a function of estimated parameters instead of constant values [34]. The ARL based on estimated parameters becomes a random variable because different samples can result in different estimated values. In such situations, the average of the ARL values namely expected average run length ($EARL$) is determined as one of the performance metrics in order to measure the effect of estimated parameters on the performance of the proposed design. Based on 10000 simulated phase-I data sets from a neutrosophic normal distribution lead to various neutrosophic control limits of the proposed control chart. This resulted in a sampling distribution of in-control \bar{ARL}_0 values which is given in Figure 5.

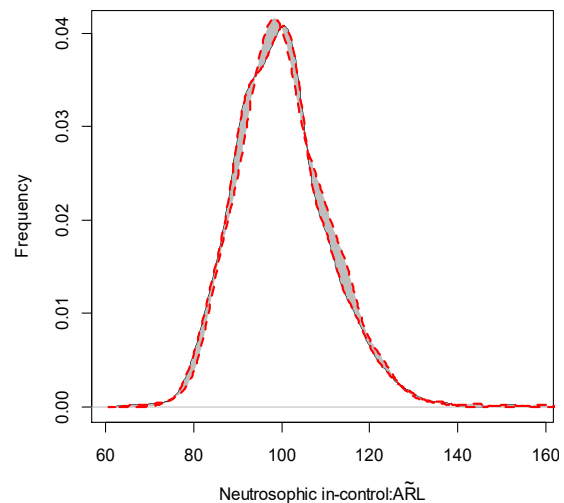
**FIGURE 5.** The density plot of \bar{ARL}_0 values for 10000 simulated \bar{MD} control charts with $\alpha = 0.01$ and $\tilde{n} \in [4, 6]$

Figure 5, shows the density plot of in-control neutrosophic \bar{ARL}_0 values, obtained from 10000 simulated \bar{MD} control charts based on $\alpha = 0.01$ and $\tilde{n} \in [4, 6]$. At the given false alarm rate $\alpha = 0.01$, the desired value of \bar{ARL}_0 is [100, 100]. It is clearly shown in Figure 5, averaging over 10000 calculated values of the neutrosophic $EARL$ values provide $EARL \in [99.12, 100.87]$ which is suitably closer to the desired value of \bar{ARL}_0 .

V. Illustrative Example

In order to demonstrate the control procedure of the new method, data from an operating manufacturing operation was utilized. Utilizing authentic data assists in developing understanding of the implementation procedure of the proposed \bar{MD} control chart. The manufacturing enterprise is Phase I database of the yogurt cup filling process [35]. The indeterminate measured data on quality characteristic of the filling process is taken in thirty groups each with five observations that are recorded in range and given in Table 4. The data from an original source are taken in exact observations at assumed target value equal to 125g. To support in understanding the preceding idea of the proposed chart, neutrosophic data are generated according procedure defined in [36]. The generated data on each studied variable are now deliberately in range instead of exact values. The proposed control chart utilizes the neutrosophic median deviation to monitor the process variability. Therefore, neutrosophic median deviation for each subgroup is computed and given in last column of the Table 4.

TABLE 4 THE IMPLEMENTATION OF PROPOSED CHART ON REAL DATA EXAMPLE

| Sample Number | \tilde{Y}_1 | | \tilde{Y}_2 | | \tilde{Y}_3 | | \tilde{Y}_4 | | \tilde{Y}_5 | | \widetilde{MAD} | |
|---------------|---------------|---------|---------------|---------|---------------|---------|---------------|---------|---------------|---------|-------------------|--------|
| 1 | [124.18 | 125.83] | [123.12 | 123.31] | [125.13 | 125.68] | [124.21 | 125.37] | [124.60 | 125.24] | [0.852 | 1.506] |
| 2 | [123.46 | 124.42] | [125.5 | 126.36] | [125.09 | 126.27] | [125.39 | 125.64] | [124.21 | 124.96] | [0.348 | 1.322] |
| 3 | [126.47 | 127.46] | [123.33 | 124.71] | [124.22 | 124.77] | [124.81 | 125.98] | [124.18 | 125.38] | [0.772 | 1.882] |
| 4 | [124.77 | 126.14] | [123.83 | 124.87] | [125.57 | 126.35] | [124.52 | 125.45] | [125.42 | 125.73] | [0.442 | 1.404] |
| 5 | [122.07 | 123.02] | [123.06 | 124.51] | [126.1 | 126.96] | [123.99 | 125.28] | [124.8 | 124.91] | [0.742 | 1.974] |
| 6 | [124.25 | 125.72] | [122.86 | 124.43] | [124.3 | 125.24] | [122.04 | 123.27] | [124.6 | 125.79] | [0.746 | 1.916] |
| 7 | [124.54 | 125.34] | [124.07 | 125.04] | [124.68 | 125.69] | [125.08 | 126.26] | [124.97 | 126.1] | [0.672 | 1.356] |
| 8 | [124.83 | 125.6] | [123.07 | 124.18] | [124.31 | 124.8] | [123.79 | 125.32] | [124.89 | 126.3] | [0.510 | 1.614] |
| 9 | [126.61 | 127.84] | [124.73 | 125.87] | [123.82 | 124.98] | [124.45 | 125.79] | [123.74 | 125.1] | [0.880 | 2.034] |
| 10 | [123.97 | 124.91] | [124.55 | 125.25] | [123.37 | 124.21] | [125.93 | 126.01] | [123.09 | 123.6] | [0.586 | 1.524] |
| 11 | [124.92 | 126.24] | [125.05 | 126.58] | [125.19 | 125.98] | [125.35 | 127.04] | [124.33 | 125.42] | [0.914 | 1.560] |
| 12 | [125.53 | 126.92] | [126.86 | 127.4] | [124.09 | 125.39] | [125.01 | 125.54] | [125.41 | 126.14] | [0.442 | 1.482] |
| 13 | [124.28 | 125.41] | [124.54 | 125.42] | [123.97 | 124.67] | [126.2 | 126.87] | [124.28 | 125.43] | [0.864 | 1.494] |
| 14 | [124.22 | 125.29] | [123.92 | 124.26] | [124.74 | 125.87] | [124.15 | 125.28] | [124.34 | 125.43] | [0.734 | 1.288] |
| 15 | [125.47 | 126.87] | [124.09 | 125.44] | [124.33 | 125.62] | [124.18 | 125.5] | [123.54 | 124.73] | [0.866 | 1.764] |
| 16 | [124.52 | 124.95] | [122.95 | 124.59] | [122.87 | 123.97] | [125.94 | 126.48] | [125.4 | 126.15] | [0.498 | 1.620] |
| 17 | [125.44 | 126.67] | [126.12 | 128.07] | [124.39 | 124.55] | [124.53 | 126.4] | [125.01 | 126.16] | [0.848 | 1.998] |
| 18 | [123.64 | 124.68] | [124.57 | 125.15] | [126.2 | 127] | [127.22 | 128.69] | [123.61 | 124.57] | [0.762 | 2.036] |
| 19 | [122.9 | 123.42] | [124.36 | 125.3] | [122.9 | 124.11] | [125.54 | 127.22] | [124.25 | 125.59] | [0.640 | 2.032] |
| 20 | [125.26 | 126.01] | [124.83 | 125.71] | [126.32 | 127.4] | [123.94 | 125.26] | [124.26 | 125.73] | [0.654 | 1.582] |
| 21 | [124.18 | 125.51] | [124.74 | 125.41] | [123.07 | 123.53] | [126.19 | 127.29] | [125.21 | 126.48] | [0.726 | 1.766] |
| 22 | [124.43 | 124.94] | [123.61 | 124.01] | [123.78 | 124.01] | [123.9 | 125.65] | [124.78 | 126.07] | [0.386 | 1.490] |
| 23 | [124.33 | 125.39] | [123.16 | 124.68] | [123.77 | 124.78] | [124.29 | 125.7] | [125.19 | 126.32] | [0.648 | 1.678] |
| 24 | [123.41 | 124.8] | [122.95 | 124.03] | [123.91 | 124.99] | [122.31 | 123.61] | [126.87 | 128.08] | [1.034 | 2.396] |
| 25 | [122.61 | 123.92] | [125.25 | 125.88] | [123.76 | 124.84] | [122.95 | 124.42] | [123.86 | 124.93] | [0.658 | 1.698] |
| 26 | [124.01 | 125.72] | [123.21 | 124.51] | [125.21 | 126.91] | [122.07 | 123.32] | [127.12 | 127.98] | [0.962 | 2.948] |
| 27 | [125.71 | 126.83] | [124.95 | 125.89] | [124.7 | 125.77] | [125.92 | 126.58] | [123.06 | 123.76] | [0.632 | 1.694] |
| 28 | [124.64 | 125.43] | [123.74 | 125.09] | [124.39 | 125.52] | [122.76 | 123.77] | [124.83 | 126.06] | [0.750 | 1.640] |
| 29 | [123.37 | 124.77] | [124.24 | 125.81] | [124.44 | 125.13] | [125.09 | 126.49] | [125.26 | 125.6] | [0.646 | 1.594] |
| 30 | [123.97 | 125.26] | [124.47 | 125.31] | [124.44 | 125.48] | [124.37 | 125.64] | [125.15 | 126.24] | [0.834 | 1.312] |

The 3-sigma control limits of the \widetilde{MD} control chart for data given in Table 3 can be obtained as:

$$UCL = [1.4895, 3.6518]$$

$$\widetilde{MD} = [0.7160, 1.7201]$$

$$LCL = [0, 0]$$

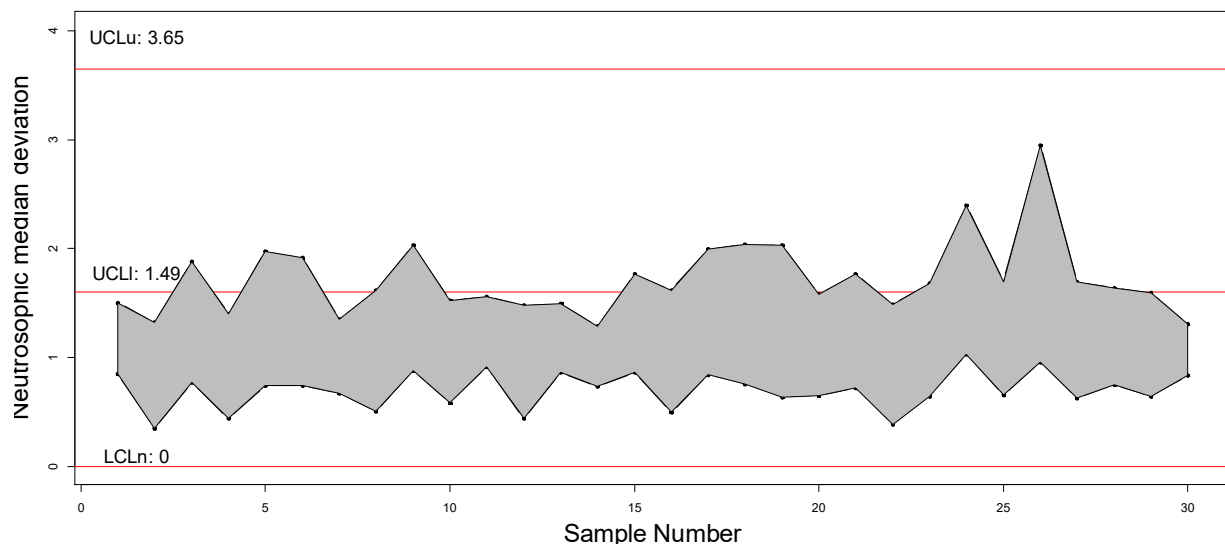
Here, the LCL is set to zero because of resulted negative values for given data at specified \tilde{n} . Whereas the

probability limits at α equal to 0.002, using (11) would lead to:

$$UCL = [1.7570, 4.2201]$$

$$LCL = [0.1305, 0.3166]$$

Both approaches provide neutrosophic probability limits that differ greatly for given data. The proposed \widetilde{MD} control chart for observed quality characteristic is schematically shown in Figure 6

FIGURE 6. The \widetilde{MD} control chart for observing the neutrosophic process dispersion parameter

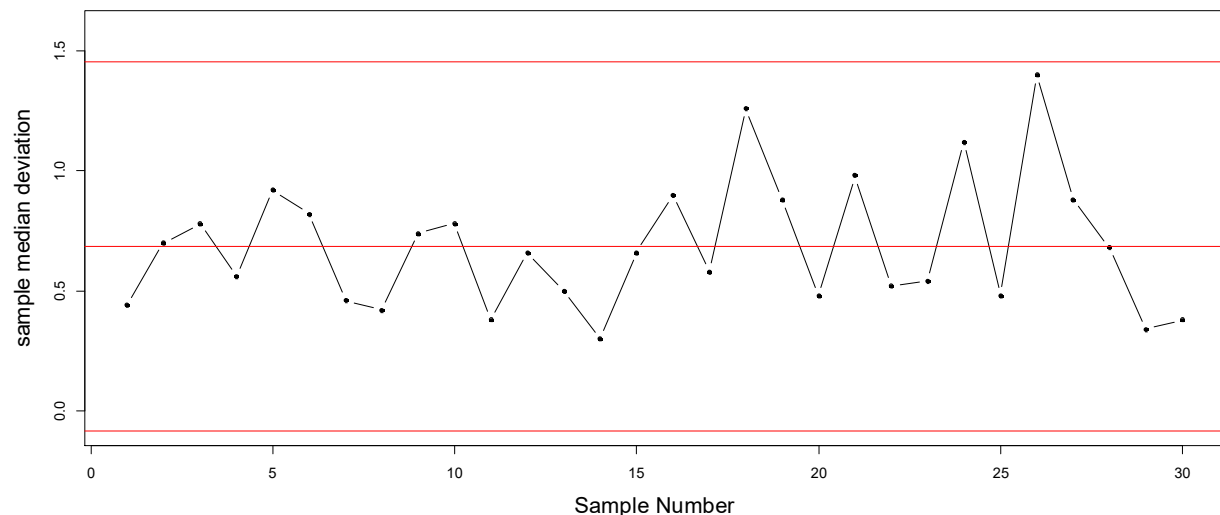


FIGURE 7. The existing MD control chart for observing the process dispersion parameter

The Figure 6 indicates that the plotted neurosophic median deviations exhibit random pattern and inside the control limits. Consequently, process may conclude as a state of in-control. In Figure 7, the conventional 3-sigma MD control chart has been set up for original data set that does not contain any indeterminacy. From this approach, similar conclusion may be inferred about the existing state of the process.

VI. CONCLUSION

In this study, a modified design of the MD control that deals with neurosophic data has been presented. To evaluate the performance of the proposed chart some related neurosophic measures as neurosophic run length (ARL), operating characteristic curve (OC) and power are developed. It has been demonstrated that how this newly design could be constructed using simulated and real-life data. Comparisons of the proposed MD control chart with other neurosophic competitor designs of R and S charts are provided. By employing a simulation study, it has been observed that proposed MD control chart considerably outperforms in terms of detecting the shift in the process as to existing neurosophic R and S control charts.

ACKNOWLEDGMENT

The authors extend their appreciation to the Deanship of Scientific Research at Majmaah University for funding this work under project number (RGP-2019-5).

REFERENCES

- [1] E. Williams, "Understanding variation-Part 2: The control chart," *Curr. Probl. Pediatr. Adolesc. Health Care*, vol. 48, no. 8, pp. 202–205, Aug. 2018.
- [2] M. P. Hossain, M. H. Omar, and M. Riaz, "New V control chart for the maxwell distribution," *J. Stat. Comput. Simul.*, vol. 87, no. 3, pp. 594–606, Feb. 2017.
- [3] L. C. E. Huberts, M. Schoonhoven, and R. J. M. M. Does, "The effect of continuously updating control chart limits on control chart performance," *Qual. Reliab. Eng. Int.*, vol. 35, no. 4, pp. 1117–1128, Jun. 2019.
- [4] M. Riaz, R. Mehmood, N. Abbas, and S. A. Abbasi, "On effective dual use of auxiliary information in variability control charts," *Qual. Reliab. Eng. Int.*, vol. 32, no. 4, pp. 1417–1443, Jun. 2016.
- [5] S.-F. Yang and B. C. Arnold, "A new approach for monitoring process variance," *J. Stat. Comput. Simul.*, vol. 86, no. 14, pp. 2749–2765, Sep. 2016.
- [6] M. Riaz and A. Saghir, "A mean deviation-based approach to monitor process variability," *J. Stat. Comput. Simul.*, vol. 79, no. 10, pp. 1173–1193, Oct. 2009.
- [7] P. J. Rousseeuw, A. M. Leroy, John Wiley & Sons., and Wiley InterScience (Online service), *Robust regression and outlier detection*. Wiley, 1987.
- [8] S. Gorard, "Revisiting a 90-year-old debate: the advantages of the mean deviation," *Br. J. Educ. Stud.*, vol. 53, no. 4, pp. 417–430, Dec. 2005.
- [9] E. Amir, and E. A. Habib "On uses of mean absolute deviation: decomposition, skewness and correlation coefficients," *METRON*, vol. 70, no. 2–3, pp. 145–164, Aug. 2012.
- [10] P. J. Huber, "Robust Statistics," in *International Encyclopedia of Statistical Science*, Berlin, Heidelberg: Springer Berlin Heidelberg, 2011, pp. 1248–1251.
- [11] M. A. Medina and E. Ronchetti, "Robust statistics: a selective overview and new directions," *Wiley Interdiscip. Rev. Comput. Stat.*, vol. 7, no. 6, pp. 372–393, Nov. 2015.
- [12] M. Schoonhoven and R. J. M. M. Does, "A robust standard deviation control chart," *Technometrics*, vol. 54, no. 1, pp. 73–82, Feb. 2012.
- [13] M. H. Shu and H.-C. Wu, "Fuzzy \bar{X} and R control charts: Fuzzy dominance approach," *Comput. Ind. Eng.*, vol. 61, no. 3, pp. 676–685, Oct. 2011.
- [14] M. Hossein, Z. Sabegh, A. Mirzazadeh, S. Salehian, and G. W. Weber, "A Literature Review on the Fuzzy Control Chart; Classifications & Analysis," *Int. J. Supply Oper. Manag.*, vol. 1, no. 2, pp. 167–189, 2014.
- [15] F. Smarandache, *A unifying field in logics : Neurosophic logic neurosophy, neurosophic Set , Neurosophic Probability (fifth edition)*, January 2005.
- [16] M. Aslam, "Introducing Kolmogorov-Smirnov tests under uncertainty: An application to radioactive data," *ACS Omega*, vol. 5, no. 1, pp. 914–917, Jan. 2020.

- [17] F. Smarandache, *Introduction to neutrosophic statistics*, Infinite Study, 2014.
- [18] M. Aslam, "A new sampling plan using neutrosophic process loss consideration," *Symmetry (Basel)*, vol. 10, no. 5, p. 132, Apr. 2018.
- [19] M. Aslam and N. Khan, "A new variable control chart using neutrosophic interval method-an application to automobile industry," *J. Intell. Fuzzy Syst.*, vol. 36, no. 3, pp. 2615–2623, Mar. 2019.
- [20] M. Aslam, N. Khan, and M. Z. Khan, "Monitoring the variability in the process using neutrosophic statistical interval method," *Symmetry (Basel)*, vol. 10, no. 11, p. 562, Nov. 2018.
- [21] M. Aslam, "Attribute control chart using the repetitive sampling under neutrosophic system," *IEEE Access*, vol. 7, pp. 15367–15374, 2019.
- [22] M. Aslam and M. A. Raza, "Design of new sampling plans for multiple manufacturing lines under uncertainty," *Int. J. Fuzzy Syst.*, vol. 21, no. 3, pp. 978–992, Apr. 2019.
- [23] M. Aslam, "Design of sampling plan for exponential distribution under neutrosophic statistical interval method," *IEEE Access*, vol. 6, pp. 64153–64158, 2018.
- [24] M. Aslam and O. H. Arif, "Testing of grouped product for the weibull distribution using neutrosophic statistics," *Symmetry*, vol. 10, no. 9, p. 403, 2018.
- [25] M. Aslam, N. Khan, and M. Albassam, "Control chart for failure-censored reliability tests under uncertainty environment," *Symmetry*, vol. 10, no. 12, p. 690, 2018.
- [26] Alhabib, Rafif, M. M. Ranna, H. Farah and A.A. Salama, "Some neutrosophic probability distributions," *Neutrosophic sets Syst*, vol. 22, pp.30-38, 2018
- [27] M. Aslam, R. A. R. Bantan, and N. Khan, "Design of a New Attribute Control Chart Under Neutrosophic Statistics," *Int. J. Fuzzy Syst.*, vol. 21, no. 2, pp. 433–440, Mar. 2019.
- [28] D. Montgomery, "Statistical quality control," 6th ed., Wiley Global Education, 2012.
- [29] S. Chakraborti, S. W. Human, and M. A. Graham, "Phase I statistical process control charts: An overview and some results," *Quality Engineering*, vol. 21, no. 1. Taylor & Francis Group, pp. 52–62, 05-Dec-2009.
- [30] M. Aslam, "Design of X-bar control chart for resampling under uncertainty environment," *IEEE Access*, vol. 7, pp. 60661–60671, 2019.
- [31] T.P. Ryan, *Statistical methods for quality improvement*, 2nd ed, John Wiley & Sons, New York, 2000.
- [32] J. Chen, J. Ye, S. Du, and R. Yong, "Expressions of rock joint roughness coefficient using neutrosophic interval statistical numbers," *Symmetry*, vol. 9, no. 7, p. 123, 2017.
- [33] A. Faraz, W. H. Woodall, and C. Heuchenne, "Guaranteed conditional performance of the S^2 control chart with estimated parameters," *Int. J. Prod. Res.*, vol. 53, no. 14, pp. 4405–4413, Jul. 2015.
- [34] N. A. Saleh, M. A. Mahmoud, L. A. Jones-Farmer, I. Zwetsloot, and W. H. Woodall, "Another look at the EWMA control chart with estimated parameters," *J. Qual. Technol.*, vol. 47, no. 4, pp. 363–382, Oct. 2015.
- [35] P. Castagliola, G. Celano, and G. Chen, "The exact run length distribution and design of the S^2 chart when the in-control variance is estimated," *Int. J. Reliab. Qual. Saf. Eng.*, vol. 16, no. 01, pp. 23–38, Feb. 2009.
- [36] P. Skrabánek and. Martínková, "Getting started with fitting fuzzy linear regression models in R," 2019.



ZAHID KHAN is an Assistant Professor in the Department of Mathematics and Statistics in Hazara University, Pakistan. He received his PhD from the University Technology PETRONAS, Malaysia in 2017. His research interests include robust estimation in nonlinear regression and statistical methods for industrial process control



MUHAMMAD GULISTAN got his MPhil degree from Quaid-e- Azam University Islamabad in 2011 and PhD degree from Hazara University in 2016. Now he is working as an assistant professor in the department of mathematics and statistics of Hazara university. His area of research is "Cubic sets and their generalizations, Non-associative hyper structures, neutrosophic cubic sets, neutrosophic cubic graphs, decision making". He published more than 60 research papers in different well reputed journals. He supervised over 25 M.Phil. and 5 PhD research students.



WATHEK CHAMMAM was born in Gabès, Tunisia, in 1980. He received the B.S degree in Mathematics from the University of Gabès, Gabès, Tunisia, in 2004, and the Master and Ph.D. degrees in Mathematics from Faculty of Science of Sfax, Sfax, Tunisia, in 2008 and 2012, respectively. In 2008, he joined the Mathematics Department of the University of Gabes as a lecturer and, in 2013, he became an assistant professor. Since September 2014, he is working with the Department of Mathematics, College of Science Zulfi, Majmaah University, KSA. His current research includes special function, Number Theory, Algebra Analysis, Theory of Fuzzy Set and Applications.



SEIFEDINE KADRY is working as an Associate Professor at Beirut Arab University, Lebanon. He received the bachelor's degree in applied mathematics from Lebanese University, in 1999, the M.S. degree in computation from Reims University, France, and EPFL, Lausanne, in 2002, the Ph.D. degree from Blaise Pascal University (France), in 2007, and the HDR degree in engineering science from Rouen University in 2017. His current research interests include education using technology, smart cities, system prognostics, stochastic systems, and probability and reliability analysis. He is a Fellow of IET, ACSIT, and ABET program evaluator.



YUNYOUNG NAM received the B.S., M.S., and Ph.D. degrees in computer engineering from Ajou University, South Korea, in 2001, 2003, and 2007, respectively. From 2007 to 2010, he was a Senior Researcher with the Center of Excellence in Ubiquitous System. From 2010 to 2011, he was a Research Professor with Ajou University. He also spent time as a Post-Doctoral Researcher at the

Center of Excellence for Wireless and Information Technology, Stony Brook University, NY, USA, from 2009 to 2013. From 2013 to 2014, he was a Post-Doctoral Fellow with the Worcester Polytechnic Institute, Worcester, MA, USA. In 2017, he was the Director of the ICT Convergence Rehabilitation Engineering Research Center, Soonchunhyang University, where he is currently an Assistant Professor with the Department of Computer Science and Engineering. His research interests include multimedia database, ubiquitous computing, image processing, pattern recognition, context-awareness, conflict resolution, wearable computing, intelligent video surveillance, cloud computing, biomedical signal processing, rehabilitation, and healthcare system.